

Analytical Methods

Accepted Manuscript



This is an *Accepted Manuscript*, which has been through the Royal Society of Chemistry peer review process and has been accepted for publication.

Accepted Manuscripts are published online shortly after acceptance, before technical editing, formatting and proof reading. Using this free service, authors can make their results available to the community, in citable form, before we publish the edited article. We will replace this *Accepted Manuscript* with the edited and formatted *Advance Article* as soon as it is available.

You can find more information about *Accepted Manuscripts* in the [Information for Authors](#).

Please note that technical editing may introduce minor changes to the text and/or graphics, which may alter content. The journal's standard [Terms & Conditions](#) and the [Ethical guidelines](#) still apply. In no event shall the Royal Society of Chemistry be held responsible for any errors or omissions in this *Accepted Manuscript* or any consequences arising from the use of any information it contains.

Cite this: DOI: 10.1039/c0xx00000x

www.rsc.org/xxxxxx

Paper

A label-free electrochemical immunosensor based on poly(thionine)-SDS nanocomposites for CA19-9 detection

Zhouqian Jiang,^{a,1} Chengfei Zhao,^{b,1} Liqing Lin,^{*a} Shaohuang Weng,^a Qicai Liu,^c and Xinhua Lin^{*a}

5 Received (in XXX, XXX) Xth XXXXXXXXX 20XX, Accepted Xth XXXXXXXXX 20XX

DOI: 10.1039/b000000x

In this paper, poly (thionine) doping sodium dodecyl sulphate nanocomposites (PThi-SDS NCs) were firstly synthesised. The morphology and characteristics of the PThi-SDS NCs were investigated by using atomic force microscopy (AFM), UV-vis spectroscopy and electrochemical methods. Owing to the unique structure and properties of PThi-SDS NCs, it was used as a redox electrochemical mediator to construct immunoassay combining gold nanoparticles (AuNPs) as the immobilization matrix for antibody. The novel biomolecular immobilization strategy based on PThi-SDS/AuNPs was used to develop a highly sensitive label-free electrochemical immunosensor for the CA19-9 detection. Under optimal conditions, the present immunosensor exhibited a wide linear range from 5 to 400 U/mL with a detection limit of 0.45 U/mL. Meanwhile, the novel immunosensor exhibited high selectivity, good reproducibility and stability.

1. Introduction

Pancreatic cancer (PC) is one of the most lethal human cancers and continues to be a major unsolved health problem.¹ The overall prognosis of pancreatic cancer is rather poor and the 5-year survival rate is as low as 3%-8%.² Since the disease has the features of high malignancy, almost all patients at diagnosis are already in an advanced stage. The poor prognosis and late presentation of pancreatic cancer patients emphasize the importance of an effective early detection strategy for patients at risk of developing pancreatic cancer. Tumor markers are used for the cancer risk estimation, early detection of the disease.³ It is reported that several tumor markers are available for screening of pancreatic cancer, especially for Carbohydrate antigen 19-9 (CA19-9). CA19-9 is an isolated Lewis antigen of the MUC1 protein, which has currently become the gold standard for pancreatic cancer diagnosis in clinical.

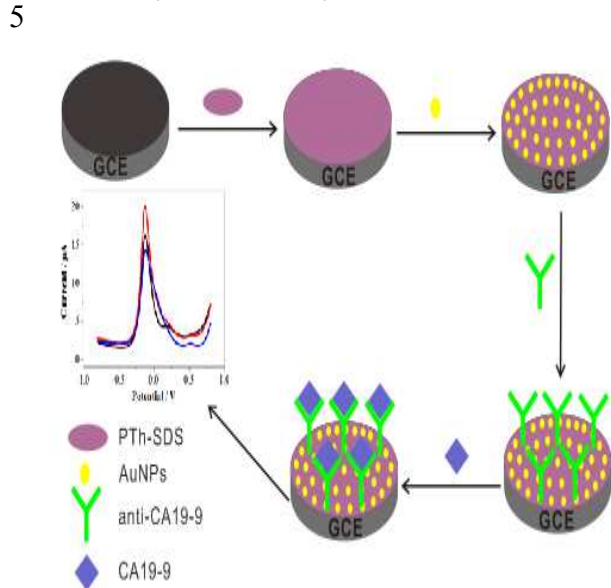
The detection of tumor markers plays an important role in initial diagnostic evaluation and follow-up examination during therapy of cancer diseases. A number of methods can be used to monitor tumor markers, such as radioimmunoassay, enzyme-linked immunosorbent assay.^{4,5} Although these methods are sensitive, they typically require labeling of the antibodies or antigens, and this makes the assay process more complex, time consuming and expensive. Among various immunoassay methods, electrochemical immunosensors have attracted considerable interest for its intrinsic advantages such as good

portability, low cost, fast analytical time, and high sensitivity.^{6,7} Electrochemical label-free immunosensors have been attracted increasing attention due to its high sensitivity, low cost and ease of preparation.

In the design and fabrication of highly sensitive electrochemical immunosensors, antibody immobilization and signal amplification are the crucial steps.⁸ Nanocomposites or hybrid materials have stimulated intense research over past decades due to their potential applications for biosensor fabrication.^{9,10} Nanocomposites with electrochemical mediators (electrochemically active compounds) have received much attention for the design and fabrication of electrochemical biosensing interfaces.^{11,12} In this perspective, various redox compounds have been adopted to fabricate electroactive nanocomposites, the representative examples are a series of redox dyes, the Prussianblue family, the ferrocene, etc.¹³⁻¹⁵

Polythionine(PThi), a stable and unique conducting polymers of phenothiazine derivatives, has been widely used for electro-analytical purposes due to high electrochemical activity toward many redox processes of small molecular compounds.¹⁶⁻¹⁷ As an attractive material, PThi can be used to directly monitor the hybridization event or construct electrochemical sensors.¹⁸ The potential incorporation of a surfactant into a conducting polymer is likely to improve the electrical, morphology, and hydrolytic stability due to the introduction of bulky hydrophobic component.¹⁹ There are no reports about SDS doping into the thionine, so this paper is trying to research whether it can improve the conductive properties and the microstructure by doping the SDS into the thionine. The positively charged thionine

1 molecules promote the ability of adsorbing SDS ions.
 2 Significantly, the PThi-SDS nanocomposites can easily form a
 3 stable thin film on glass carbon electrode (GCE) with efficient
 4 redox-activity and conductivity.



6 Scheme 1 Schematic illustration of the label-free electrochemical
 7 immunoassay protocol for detection of CA19-9.

10 In this paper, a facile, novel biomolecular immobilization
 11 strategy based on PThi-SDS/AuNPs was used to develop a highly
 12 sensitive label-free electrochemical immunosensor for the
 13 CA19-9 detection. PThi-SDS NCs were synthesised and used for
 14 fabrication of label-free electrochemical immunosensor. The
 15 immunosensor working principle and manufacturing process are
 16 shown in Scheme 1. First, PThi-SDS NCs was prepared and
 17 immobilized onto a bare GCE, AuNPs was dropped on the
 18 PThi-SDS NCs modified electrode. Then the anti-CA19-9 was
 19 immobilized on modified GCE surface. AuNPs are well-known
 20 bio-nanomaterials because of their large specific surface area,
 21 strong adsorption ability, well suitability, and good
 22 conductivity.^{20, 21} It can strongly interact with biomaterials and
 23 has been utilized as an intermediary to immobilize antibody to
 24 efficiently retain its activity and to enhance current response in
 25 the construction of immunosensor.²² Thus, when incubated with
 26 CA19-9, the formation of a non-conducting immunocomplex
 27 towards CA19-9 through immunoreaction will reduce the
 28 response of the constructed electrochemical loop containing
 29 PThi-SDS NCs layer. Then, the modified electrode was placed in
 30 an electrochemical detector cell containing pH5.5 PBS solutions
 31 to record the electrochemical signals. The reduced current before
 32 and after the formation of immunocomplex corresponds to the
 33 concentration of CA19-9.

34 2. Experimental

35 2.1 Chemicals and instruments

Carbohydrate antigen 19-9 (CA19-9) was purchased from Tosoh
 Company. Carbohydrate antibody 19-9 (anti-CA19-9) was
 purchased from Abcam Company. HNO₃, H₂O₂, ethanol,
 NaH₂PO₄•2H₂O, Na₂HPO₄•12H₂O, NaOH, NaCl, H₂SO₄, HCl,
 40 H₃PO₄, HAuCl₄•4H₂O, K₄[Fe(CN)₆]•3H₂O, K₃[Fe(CN)₆], KCl
 and FeCl₃•6H₂O were obtained from Sinopharm Chemical
 Reagent Co., Ltd., These reagents were of analytical reagent
 grade. Thionine acetate was purchased from Sigma-Aldrich
 company.

45 Phosphate buffer saline (PBS, pH=4.0, 4.5, 5.0, 5.5, 6.0, 6.5,
 7.0) acted as the electrolyte solution containing 100 mM
 NaH₂PO₄-Na₂HPO₄ and 100 mM NaCl and adjusting its pH with
 H₃PO₄ solution and NaOH solution. All the experimental solution
 was stored in a refrigerator (4°C) when not used. In all the
 50 procedures, the ultrapure water with a specific resistance of 18.2
 MΩ•cm was prepared with Milli-Q-purified system. UV-vis
 absorption spectra were recorded using a UV-2250 UV-vis
 spectrophotometer (Shimadzu, Japan). Atomic force microscopy
 (AFM) images were collected using a Bruker Multimode 8 SPM
 55 system in tapping mode. All electrochemical experiments were
 measured on a CHI660C electrochemical workstation (Shanghai,
 China). A three-electrode electrochemical cell was composed of a
 modified glass carbon electrode (GCE, Φ=3mm) as the working
 electrode, a platinum wire as the auxiliary electrode, and a
 60 Ag/AgCl electrode as the reference electrode.

2.2 Preparation of AuNPs and PThi-SDS NCs

The AuNPs with sizes of 13 nm used in this work were prepared
 according to the
 literature.²³

65 With some modifications of the literature,²⁴ in brief, 0.03 g
 FeCl₃ was dissolved in 50 mL of water in a 100 mL two-neck
 glass reactor, and then 0.08 g of thionine monomer was added
 while stirring (300 rpm) vigorously at 50°C. Later, 0.05 mM SDS
 was added. After that, 200 μL 30% H₂O₂ solution were added and
 70 refluxed for 24 h. The brown precipitate of PThi-SDS NCs were
 collected by centrifuging at 5000 rpm and then repeatedly washed
 with 0.1 M HCl and deionized water to remove residual ions and
 monomer. It was vacuum dried overnight at 40°C. The collected
 samples were re-dispersed in N,N-dimethylformamide (DMF) to
 75 be 4 mg/mL for subsequent use.

2.3 Fabrication of the label-free electrochemical immunosensor

Prior to experiment, the glass carbon electrode(GCE, Φ=3 mm)
 was carefully polished with 1.0, 0.3 and 0.05 μm alumina
 80 powder separately, followed by successive sonication in HNO₃
 solution(HNO₃ : H₂O =1:1), absolute ethyl alcohol and double
 distilled water for 5 min and dried in nitrogen. Then 2.5 μL
 PThi-SDS composites solution was casted onto the clean GCE
 and dried at room temperature. Then, AuNPs was dropped on the
 85 PThi-SDS NCs modified GCE. The obtained electrode was
 incubated in 100 μg/mL anti-CA19-9 at 37°C for 1 h and then

blocked with 1% BSA, after thoroughly rinsed with PBS and dried in nitrogen, the modified GCE was noted as anti-CA19-9/AuNPs/PThi-SDS/GCE. The prepared GCE was

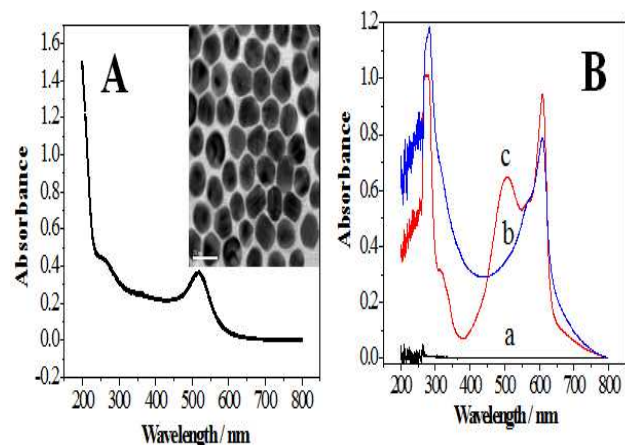


Fig. 1 Uv-Vis absorption spectra of the AuNPs. The inset shows the TEM image of the AuNPs(A); Uv-Vis absorption spectra of SDS (a), thionine (b) and PThi-SDS (c) in DMF(B).

incubated in various concentrations of CA19-9 for 1 h at 37°C to obtain CA19-9/anti-CA19-9/AuNPs/PThi-SDS/GCE, then washed by PBS and dried in nitrogen. After every modified step, the electrode was placed in an electrochemical detector cell containing pH5.5 PBS solutions to record the electrochemical signals.

2.4 Electrochemical measurements

A conventional three-electrode system composing of the work electrode (modified GCE), reference electrode (Ag/AgCl electrode) and auxiliary electrode (platinum wire) was used for all the electrochemical detections. The differential pulse voltammetry (DPV) and cyclic voltammetry (CV) were performed on CHI660C electrochemical workstation (Shanghai, China) in the PBS solution. Electrochemical impedance spectroscopy (EIS) was carried out on an Autolab PGSTAT302N system in the PBS solution containing 10 mM $[\text{Fe}(\text{CN})_6]^{3-}/[\text{Fe}(\text{CN})_6]^{4-}$ and 0.1 M KCl.

3. Results and discussion

3.1 Characterization of AuNPs and PThi-SDS nanocomposites

Fig. 1A shows the typical UV-vis absorption spectra of the AuNPs. AuNPs exhibit a 520 nm of characteristic absorption peak. It can be seen from the inset image of TEM that gold nanoparticles with uniform sizes of around 13 nm. Fig. 1B shows the UV-vis absorption spectra of SDS (curve a), thionine monomer (curve b) and PThi-SDS NCs (curve c) in DMF solvent. There is no absorption peak for SDS dissolved in DMF.

The absorption bands of PThi-SDS NCs (280, 316, 567 and 610 nm) were generally similar to those of thionine (283, 318, 563 and 606 nm). The absorption bands at 283 and 318 nm were attributed

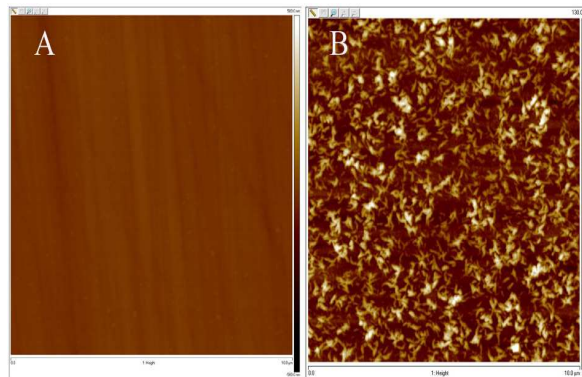


Fig. 2 AFM images of bare GCE (A) and PThi-SDS/GCE (B).

to the $\pi-\pi^*$ transition of a phenothiazine ring and the $n-\pi^*$ transition of an amine group, respectively.²⁵ A rise of the absorbance at 610 nm is observed with a bathochromic shift due to interactions between the SDS and poly(thionine). The new absorption band that appeared at 507 nm was possibly due to SDS as a counter-ion doping into poly(thionine), directly affect the state of aggregation and charge transfer between molecular chains of poly(thionine), finally make the structure of poly(thionine) change. This indicates that PThi-SDS NCs was obtained successfully by the oxidation of the monomer thionine doping SDS.

To further verify the successful synthesis of PThi-SDS NCs, AFM images of the nanostructures were investigated. Fig. 2 shows the typical AFM of bare GCE (Fig.2A) and PThi-SDS NCs (Fig. 2B). The bare GCE maintains a smooth and flat surface. The surface of PThi-SDS NCs modified electrode appears uniform granular nanostructure and evenly distributed.

3.2 Electrochemical characterization of PThi-SDS NCs

To clarify the effect of SDS for the property of PThi-SDS NCs, we tested the electrochemical response of same procedure of the immobilization of PThi and PThi-SDS NCs on the surface of

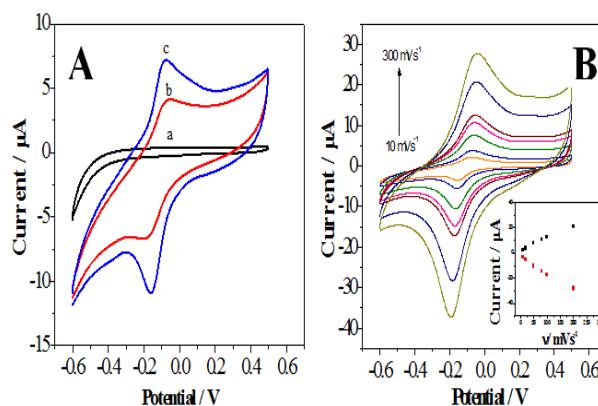


Fig. 3 CVs of bare GCE (a), PThi (b) and PThi-SDS NCs (c) in 0.1 M pH 5.5 PBS(A); CV studies of PThi-SDS/GCE electrode as a function of scan rate (10-300 mV/s). The inset shows the image of peak current and scan rate(B).

GCE, respectively. The CVs experiment were performed to investigate whether or not the present SDS improves the electron transfer. As shown in Fig. 3(A), there is no a pair of redox peaks on the bare GCE (curve a). When the PThi immobilized onto surface of GCE, the current response increased obviously with a pair of peaks. The peak separation (ΔE_p) is about 150 mV for the PThi. Compared with PThi, immobilized PThi-SDS NCs indicated drastically increased current response and lower separation of ΔE_p (112 mV, curve c), obviously indicating the improved electron transfer. The significantly enhanced current response could be attributed to the fact that SDS doped into poly(thionine) as a counter-ion. In general, poly(thionine) is positively charged and SDS is negative, SDS possesses nucleophilic and electronegative characteristics and directly affected the state of aggregation and charge transport between the molecular chain of poly(thionine). And ultimately affect the conductive performance of PThi-SDS NCs.

The CVs of the modified electrode in pH 5.5 PBS at different scan rate were shown in Fig. 3(B). The anodic and cathodic peak current increased with the increase of scan rate in the range of 10-300 mV/s. Also, the I_{pa} and I_{pc} showed a linear relationship with the scan rate respectively in the range of 10-300 mV/s (the inset of Fig.3B), suggesting that the electrode reaction is a surface-controlled electrochemical process, indicating that the changes of the electrode surface can regulate the signal response of PThi-SDS NCs.

The effect of pH at the PThi-SDS/GCE electrode also studied, as shown in Figure S1. In the range of 4.0-7.0, with increasing the pH, both the E_{pa} and the E_{pc} shifted negatively. The values of E^0 , which was dependent on the pH value, show that the redox couple of the PThi-SDS includes proton transfer in the redox processes (the inset of Fig. S1). According to the Nernst equation, the slope of -56.2 mV pH^{-1} reveals that the proportion of the electron and proton involved in the reaction is 1:1.

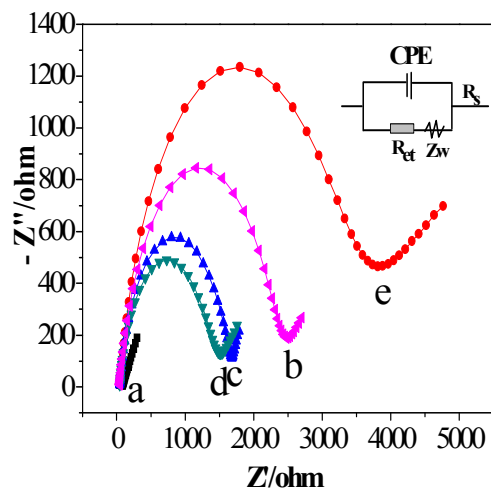


Fig. 4 EIS of the fabrication progress of the immunosensor. GCE (a); PTh-SDS/GCE (b); AuNPs/PTh-SDS /GCE (c); anti-CA19-9/AuNPs/PTh-SDS/GCE(d) and CA19-9 /anti-CA19-9 /AuNPs /PTh-SDS/GCE (e).

3.3 Electrochemical characterization of the immunosensor

In order to characterize the fabrication process of the immunosensor, EIS were recorded at each immobilization step and shown in Fig. 4. EIS was performed to provide the interfacial properties of different stepwise of modified GCE in 10 mM $[\text{Fe}(\text{CN})_6]^{3-}/[\text{Fe}(\text{CN})_6]^{4-}$ and 0.1 M KCl from 0.1 Hz to 100 kHz. The EIS of bare GCE shows an nearly straight line (curve a), indicating that diffusion process dominates. Then PThi-SDS NCs was immobilized on the bare GCE. The EIS appeared evidently semicircle part, the electron transfer resistance (R_{ct}) of which was about 2500 Ω (curve b). The reason mainly is that PThi-SDS NCs hinder the $[\text{Fe}(\text{CN})_6]^{3-/4-}$ reach to the electrode surface occur redox reaction. After AuNPs were doped on modified electrode, the R_{ct} greatly decreased to be about 1700 Ω (curve c), indicating that AuNPs can improve the electron transfer. When anti-CA19-9 was adsorbed onto the electrode, the R_{ct} value further decreased to be about 1500 Ω (curve d). This is maybe that H^+ plays a greater effect in PThi-SDS NCs than the protein spatial structure on signal. Electrostatic adherence between $[\text{Fe}(\text{CN})_6]^{3-/4-}$ and positive anti-CA 19-9 reduced the R_{ct} value. Finally, when CA19-9 was captured through immunoreaction, non-conductive and negative CA19-9 would go against the transfer of $[\text{Fe}(\text{CN})_6]^{3-/4-}$ on modified GCE and make the R_{ct} obvious increase to be about 3900 Ω (curve e). The results of EIS suggested that stepwise modification of GCE was successful.

3.4 Optimization of experimental conditions

Since the pH buffer would influence the electrochemical response of PThi-SDS, thus the pH of detecting buffer was investigated at first. As shown in Fig. S2, the maximum value of ΔI was appeared at pH 5.5. Therefore, the pH 5.5 was adopted for following experiment. The reaction temperature of antigen-antibody could severely influence the amount of CA19-9 immobilized on the modified GCE. As depicted in Fig. S3, the current value separation (ΔI) rapidly increased from 20°C to 37°C, reached the maximum value at 37°C and then decreased with the temperature over 37°C. Therefore, 37°C was adopted as the optimal reaction temperature of antigen-antibody. Incubation time also affected the performance of the immunosensor. Hence, the incubation time was also investigated in Fig. S4. The changeable current (ΔI) rapidly increased with the incubation time, and tended to level off after 60 min, indicating a saturated formation of the immunocomplex. Therefore, 60 min was selected as the incubation time for the immunoassay.

3.5 The performance of the immunosensor

To evaluate the performance of the immunosensor, anti-CA19-9/AuNPs/PThi-SDS/GCE was exposed to various concentrations of CA19-9 solutions under optimized conditions. Before and after the antigen CA19-9 with different concentrations reacted with anti-CA19-9/AuNPs/PThi-SDS/GCE, DPVs were

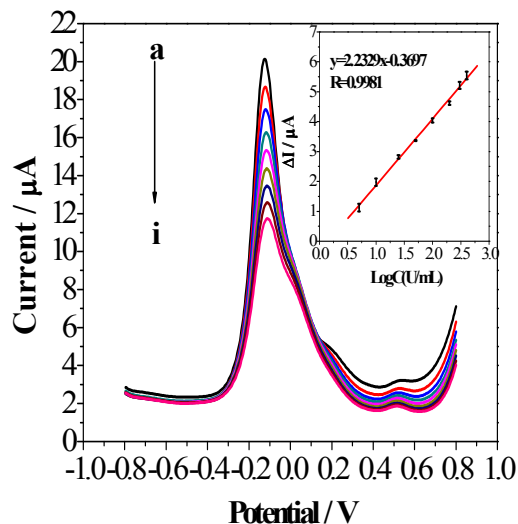


Fig. 5 DPVs of the immunosensor incubated with different concentrations of CA19-9 standard solution (from a to i): 0.0, 5.0, 10.0, 50.0, 100.0, 200.0, 300.0 and 400.0 U/mL in 0.1 M pH 5.5 PBS. Inset shows the calibration plots of the oxidation current change (ΔI) versus concentration of CA19-9 under optimal conditions.

collected. As shown in Fig. 5 the peak currents obtained after the antigen-antibody reaction decreased with the increment of CA19-9 concentration, which is caused by the increased hindrance of the immunocomplex to electron-transfer of PThi-SDS mediator. The electrochemical signal decreased was proportional to CA19-9 concentration in the range of 5–400 U/mL. The detection limit of 0.45 U/mL ($S/N=3$).

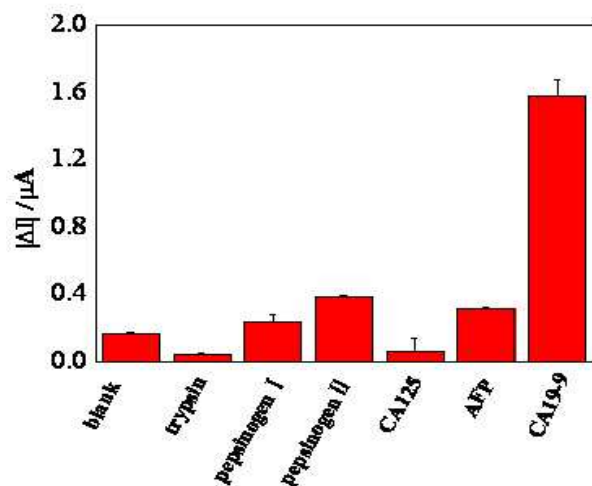


Fig. 6 Selectivity investigation of the label-free electrochemical immunosensor for CA19-9 (0 U/mL), trypsin (5 ng/mL), pepsinogen I (5 ng/mL), pepsinogen II (5 ng/mL), CA125 (5 ng/mL), AFP (5 ng/mL) and CA19-9 (5 U/mL), the error bars represent the standard deviation of three measurements.

3.6 Selectivity, reproducibility and stability

Selectivity is one of the main advantages of using biological molecules as recognition elements in immunosensor. In order to investigate the specificity of this immunosensor, trypsin, pepsinogen I, pepsinogen II, cancer antigen 125 (CA125) and alpha-fetoprotein (AFP) were selected as the predominant interferences. The result was shown in Fig. 6. Compared to the result obtained from the only CA19-9 (5 U/mL), the change of current response of the immunosensor before and after incubation with 5 ng/mL trypsin, pepsinogen I, pepsinogen II, CA125 and AFP were weak. All these results clearly demonstrated the high selectivity of this immunoassay.

Reproducibility was also a very important feature for immunosensor, and it was necessary to check it to confirm the reliability of this developed immunosensor. The reproducibility of the current response of the immunosensor was investigated by analysis of the same concentration of CA19-9 (100 U/mL) using five equally prepared electrodes. The five electrodes exhibited the similar electrochemical responses and a relative standard deviation (RSD) of 4.8% was obtained, indicating satisfying reproducibility.

The stabilities of the proposed immunosensor were researched by long-term storage assay. The long-term storage stability was investigated over a period of 20 days of storage (at 4°C). The DPV peak current of the immunosensor decreased gradually and retained 91.3% of its initial current after the first 10 days storage and 88.6% after 20 days storage. These results indicated that the stability of the immunosensor was satisfactory in this experiment. We speculate that the long-term stability mainly attributed to the following issue: AuNPs with large surface area and good affinity for biomolecules ensure the stability of antibody on the electrode surface.

4. Conclusions

In the present paper, we report on the fabrication of highly sensitive and label-free electrochemical immunosensor based on immobilization of antibody molecules on biocompatible PThi-SDS/AuNPs nanocomposite film. The PThi-SDS NCs were synthesized by a simple chemical polymerization method. The PThi-SDS NCs could avoid the leakage of Thi from the matrix and retain its electrochemical activity. The present immunosensor exhibited high selectivity and a wide linear range from 5 to 400 U/mL with a detection limit of 0.45 U/mL. This immunosensor provides potential applications for clinical immunoassays.

We gratefully acknowledge the financial support of the National High Technology and Development of China (863

Project: 2012AA022604), the National Natural Science Foundation of China (21275028, 81171668 and 20975021), the Fujian provincial health system backbone talents cultivate Program (2014-ZQN-JC-23), the Fujian Provincial University-Industry Cooperation Science & Technology Major Program (2010Y4003), the Scientific Research Major Program of Fujian Medical University (09ZD013).

Notes and references

- a. Department of Pharmaceutical Analysis, School of Pharmacy, Fujian Medical University, Fuzhou 350108, China
 - b. Pharmaceutical and Medical Technology College of Putian University, Putian 351100, China
 - c. Department of Laboratory Medicine, First Affiliated Hospital of Fujian Medical University, Fuzhou 350005, China
- 1: These authors cotributed equally.
Corresponding author E-mail address: Liqing Lin: fjmulinliqing@gmail.com, Tel./fax: +86 591 22862016.
Xinhua Lin: xhl1963@sina.com. Tel./fax: +86 591 22862016.
Electronic Supplementary Information (ESI) available: [details of any supplementary information available should be included here]. See DOI: 10.1039/b000000x/
- 1 D. Li, K. Xie, R. Wolff and J.L. Abbruzzese, *Lancet*, 2004, **363**, 1049.
 - 2 N. Bardeesy and R.A. DePinho, *Nature Rev Cancer*, 2002, **2**, 897.
 - 3 G.L. Perkins, E.D Slater, G.K. Sanders and J.G. Prichard, *Am Fam Physician*, 2003, **68**, , 1075.
 - 4 P. Eric, C. Amel and S. Toihiri, *Clin. Chem. Lab. Med.*, 2014, **52**, 437.
 - 5 J. Wu, J. Tang, Z. Dai, F. Yan, H. Ju and E. N. Murr, *Biosens. Bioelectron.*, 2006, **22**, 102.
 - 6 G.A. Crespo, G. Mistlberger and E. Bakker, *J. Am. Chem. Soc.*, 2012, **134**, 205.
 - 7 M. Chen, C. Zhao, W. Chen, S. Weng, A. Liu, Q. Liu, Z. Zheng, J. Lin and X. Lin, *Analyst*, 2013, **138**, 7341
 - 8 S. Sanchez, M. Roldan, S. Perez and E. Fabregas, *Anal.Chem.*, 2008, **80**, 6508.
 - 9 R. Hao, R.J. Xing, Z.C. Xu, Y.L. Hou, S. Gso and J.S. Sun, *Synthesis, Advanced Materials*, 2010, **22**, 2729.
 - 10 P. Jing, W. Xu, H. Yi, Y. Wu, L. Bai and R. Yuan, *Analyst*, 2014, **139**, 1756.
 - 11 S. M. Bromfield, A.Barnard, P. Posocco, M. Fermeglia, S. Pricl and D.K. Smith, *J. Am. Chem. Soc.*, 2013, **135**, 2911.
 - 12 Y. Zhuo, Y.P.X. uan, R. Yuan, Y.Q. Chai and C.L. Hong, *Biomaterials*, 2008, **29**, 1501.
 - 13 X.F Liu, L.O. Yang, X.H. Cai, Y.Q Huang, X.M. Feng, Q.L. Fan and W. Huang, *Biosens. Bioelectron.*, 2013, **41**, 21.
 - 14 Z.J. Wang, M.Y.Li, Y.J. Zhang, J.H. Yuan, Y.F. Shen, L. Niu and A. Ivaska, *Carbon*, 2007, **45**, 2111.
 - 15 H. Wang, H. Ohnuki, H. Endo and M. Izumi, *Bioelectrochemistry*, 2015, **101**, 1.
 - 16 J.M Han, J. Ma and Z.F. Ma, *Biosens.Bioelectron.* 2013, **47**, 243.
 - 17 A. J. S. Ahammad, M. M. Rahman, G. R. Xu, S. Kim and J. J. Lee, *Electrochim. Acta*, 2011, **56**, 5266.
 - 18 N. Zhang, K.Y. Zhang, L. Zhang, H.Y Wang, H.W. Shi and C. Wang, *Anal Methods*, 2015, **7**, 3164.
 - 19 M. Omastova, M. Trchova, J. Kovarova, *J. Stejskal and S. Metals*, 2003, **138**, 447.
 - 20 Z.J. Song, R. Yuan, Y.Q. Chai, B. Yin, P. Fu and J.F. Wang, *Electrochimica Acta*, 2010, **55**, 1778.
 - 21 L.Q. Lin, A.L. Liu, C.F. Zhao, S.H. Weng, Y. Lei, Q.C. Liu, X.H. Lin and Y.Z. Chen, *Biosens. Bioelectron.*, 2013, **42**, 409.
 - 22 K.J. Huang, J. Li, Y.Y. Wu and Y.M. Liu, *Bioelectrochemistry*, 2013, **90**, 18.
 - 23 L.Q. Lin, S.H. Weng, C.F. Zhao, Q.C. Liu, A.L. liu and X.H. Lin. *Electrochimica Acta*, 2013, **108**, 808.
 - 24 N. C. Deb Nath, S. Sarker, M. M. Rahman, H. J. Lee, Y. J Kim and J.J. Lee, *Chemical Physics Letters*, 2013, **559**, 56.
 - 25 Y.B. Shim and J.H. Park, *J. Electrochem. Soc.* 2000, **147**, 381.